Scientific Herald of Uzhhorod University
Series “Physics”

Journal homepage: https://physics.uz.ua/en
Issue 49, 9-18
Received: 12.01.2021. Revised: 15.03.2021. Accepted: 25.05.2021

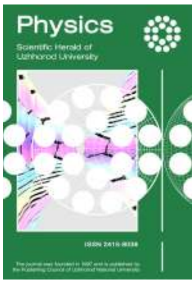

УДК 543.429.22
PACS 61.43. Gt, 61.46. Hk, 81.05. Cy, 81.05. Rm, 81.07. Bc, 81.07. Wx, 81.20.Fw
DOI: 10.24144/2415-8038.2021.49.9-18

EPR-Spectral, Magnetic, and Ionic Features of CeO_2, Yb_2O_3, Yb_2O_3-CeO_2 Powders and Ceramics Based on REO Oxides

Yurii M. Bataiev, Mykola M. Bataiev, Oksana A. Kornienko, Olena M. Lavrynenko, Olesia Yu. Pavlenko*

Frantsevych Institute for Problems of Material Science of NASU
03142, 3 Krzhyzhanovskii Str., Kyiv, Ukraine

Abstract

Relevance. The nature and properties of rare earth oxides affect the dynamics of magnetisation and surface magnetic properties of the obtained ceramic materials. The electron paramagnetic resonance lines and the dynamics of their intensity help understand the physical and chemical changes of oxides during heat treatment. They are also responsible for the corresponding ionic form, the crystalline form of the oxide, and the magnetic features.

Purpose. To study the mechanism of formation of paramagnetic centres (using Yb^{3+} and Ce^{4+} ions), as well as the effect of temperature on the processes of thermal generation.

Methods. The method of electron paramagnetic resonance spectroscopy was used. The mathematical processing of the electron paramagnetic resonance line is shown using the theoretical Lorentz model.

Results. The electron paramagnetic resonance spectra for rare earth oxides indicate that heat treatment from 120 °C to 1500 °C leads to a change in intensity, a change in the position of spectral lines and a modification of the value of the g-factor. Heat treatment of oxide samples leads to a redistribution of the EPR spectral features and properties of oxides and a predominance of features with corresponding discrete and continuous values.

Conclusions. The heights of the lines and the area under the curves of the calcined Yb_2O_3 samples show a linear increase in the structural rearrangement together with an increase in the number of magnetic domains. The electron paramagnetic resonance spectra of the initial Yb_2O_3-CeO_2 oxide mixture show changes in the spectroscopic features and the formation of Yb^{3+} cations

Keywords: rare earth oxides, REOs, EPR spectroscopy, magnetisation dynamics, magnetic properties

Introduction

Materials based on cerium oxides and lanthanides are widely used in high-tech industries. In recent years, cerium dioxide has been used as protective coating that absorbs UV radiation, as a major component of polishing mixtures and abrasives and nanoelectronics in sensor devices [1] that allow determining the minimum number of impurities in gas mixtures, electrochromic coatings, etc. Highly dispersed cerium dioxide and solid solutions based on it are part of three-way catalysts designed for efficient combustion of automobile exhaust gases, used in selective oxidation reactions in the dehydrogenation of alcohols, etc. [2-4].

Significant interest in materials based on CeO_2 in recent years exists because transition to the nanocrystalline state changes its physicochemical features. Cerium dioxide is used in biomedicine [5; 6]. For example, the introduction of a small amount of cerium dioxide into the retina significantly reduces the negative effects of UV radiation on photoreceptor cells, and $CeO_{2-\delta}$ nanoparticles significantly increase the viability of brain cells [1]. Cerium nanocrystals of CeO_{2-x} were among the first to show activity similar to the activity of enzymes in a living cell [7]. They still remain one of the most promising materials both in terms of the diversity of possibilities for the

Suggested Citation:
Bataiev YuM, Bataiev MM, Kornienko OA, Lavrynenko OM, Pavlenko OYu. EPR-spectral, magnetic, and ionic features of CeO_2, Yb_2O_3, Yb_2O_3-CeO_2 powders and ceramics based on REO oxides. *Scientific Herald of Uzhhorod University. Series “Physics”*. 2021;(49):9-18.

*Corresponding author

implementation of their anti-/prooxidant activity, and in terms of the number of biomedical studies conducted with these nanoparticles [7]. The prospects for the use of cerium dioxide in biomedicine are related to two main factors: low toxicity and high oxygen non-stoichiometry.

Additional oxygen non-stoichiometry can be achieved by doping CeO_2 elements with an oxidation state of 3+, in particular oxides of rare earth elements, which also leads to an increase in the biological activity of cerium dioxide-based materials. Solid solutions based on CeO_2 are characterised by high ionic conductivity [5-8] and absence of phase transitions in a wide temperature range [9; 10]. Therefore, they are the most promising electrolytes operating at moderate temperatures, because their ionic conductivity and sensitivity to oxygen partial pressure are much higher than that of ZrO_2 stabilised by Y_2O_3 (YSZ) [11]. One of the methods that allowed obtaining detailed information about the local properties of nanosized materials was electronic paramagnetic resonance (EPR).

Temperature treatment of mixtures of rare earth oxides (REOs) is widely used to create various functional materials for technical purposes. Typically, the nature of the REO, the phase composition of the source powders, the mode of their dispersion, the sintering temperature and the crystal structure of the obtained ceramics significantly influence the dynamics of magnetisation and surface magnetic properties of the obtained ceramic materials [12-16]. EPR lines and changes in intensity allows interpreting the physical and chemical changes in the oxide during heat treatment, which are responsible for the corresponding ion form, the crystalline form of the oxide and the magnetic features of the oxide [13-16]. A suitable form of the ion includes an ion in the substitution position in the crystal lattice of the oxide, an ion in the internodes in the oxide lattice and an ion in the impurity position. The spectral features of EPR spectroscopy allowed concluding on the mathematical model used and applied upon shaping the line in the spectrum and the spectral features of samples based on oxides (REO). The corresponding mathematical model contains the use of functions of Gaussian curves, Lorentz and Pearson functions, inverse polynomial and mathematical models of Voigt. The comparative features of these mathematical models include complex spectrum processing and allowed predicting the highest quality and best model for the corresponding line in the spectrum of oxides (REOs).

When using the EPR spectroscopy method, additional mathematical models are used for centres of low symmetries, for fine and ultrafine structure in spectra, for quadrupole interaction, for spin-orbit and spin-spin relaxation physical models. The application of these models in the calculations of experimental data allows drawing additional conclusions about the appropriate configuration of ions and the structure of ions in crystal fields. The values of the spin-orbital and spin-spin parameters and their features allows drawing practical conclusions about the ion configuration in oxides of rare earth elements (REOs) [17-19].

The EPR lines and changes in intensity allow interpreting the physical and chemical changes in the oxide upon heat treatment. These changes are responsible for the corresponding ion form, the crystalline form of the oxide, and the magnetic features of the oxide. A suitable form of the ion includes an ion in the substitution position in the crystal lattice of the oxide, an ion in the internodes in the oxide lattice and an ion in the impurity position. The corresponding value of the g-factor for the EPR lines in the spectrum allows drawing conclusions about the shape of the ion and its location in the crystal lattice.

The crystalline form of the oxide consists of a cubic, rhombic, trigonal, tetragonal, or hexagonal shape. The value of the g-factor for the lines in the EPR spectrum and their relative ratio allows concluding on and interpreting the shape of the oxide for the corresponding ion. The intensity of EPR lines allows finding the relative and absolute concentration of spins in the form of the corresponding oxide and predicting their magnetic properties and features. The magnetic features of the oxide lie in the superposition of the corresponding magnetic and spectral features of this oxide material. The corresponding value of the intensity of the EPR line and the value of the g-factor suggest an unambiguous conclusion about the magnetic features of this material. The EPR spectra show lines related to the paramagnetic, ferromagnetic, and ferrimagnetic features of the respective material [13; 16; 20].

The value of the shift in the EPR spectrum for oxides (REOs) involves the use of a model of chemical and Knight's shift of the spectral line to the corresponding oxide. Quantum-mechanical calculations lead to the conclusion that the line shift according to the theory leads to additional changes in the value of electronic magnetic susceptibility and the value of electronic magnetisation. The value of the Knight's shift is at the same time linearly dependent on the value of the mass of the atom or the mass of the ion of oxides of rare earth elements (REOs). For crystals with axial symmetry, the Knight's shift is dependent on the angle between the axis of symmetry of the crystal and the magnetic field. The angular dependence of the value of the Knight's shift with the corresponding theoretical model allows finding the parameters of magnetic susceptibility and electronic magnetisation of the material.

The purpose of this study was to investigate the formation mechanism of paramagnetic centres with the use of Yb^{3+} and Ce^{4+} ions; to study the temperature effect on the thermogeneration processes of these paramagnetic centres.

Materials and Methods

Industrial oxides of cerium and ytterbium were used for the study, based on which mixtures with a weight ratio of 95 wt.% Yb_2O_3 to 5 wt.% CeO_2 were made. The individual oxides CeO_2 and Yb_2O_3 were compared. The starting components were mixed in a ball mill for 2 h in the presence of ethanol. The dispersed powders were compressed into tablets with a diameter of 5 mm and a height of 4 mm under a pressure of 13.3 MPa and sintered in an oven at temperatures of 1100 °C and 1500 °C for 10 and 50 hours. Experimental measurements were performed on a spectrometer Radiopan 2547 SE/X, equipped with a resonator type RCX660A, electromagnet ER 2505 and a high-frequency unit MS212 with a frequency of 9.3 GHz. Glass tubes were applied to perform EPR measurements. The cryostat module of liquid nitrogen was used to measure temperature dependences in the range from 77 to 300 K [21; 22]. The obtained results indicated a good correspondence of the theoretical model for EPR spectra. To obtain REOs mixtures, the following ratio of oxides was chosen: 90 mol.% Yb_2O_3 to 10 mol.% CeO_2. The starting components were mixed in a ball drum for 2 hours. The powders were compressed into tablets with a diameter of 5 mm and a height of 4 mm under a pressure of 13.3 MPa and sintered in an oven at temperatures of 1100 °C and 1500 °C for 10 hours.

The method of electron paramagnetic resonance (EPR) spectroscopy was used to study the initial oxides of CeO_2, Yb_2O_3, CeO_2-Yb_2O_3 mixtures and ceramics based on them obtained at temperatures of 1100 °C and 1500 °C. Magnetic and spectral parameters, cerium and ytterbium and ceramics based on their mixture are studied. Mathematical processing of EPR lines is performed by using a theoretical Lorentz model. Line width measurements are performed according to the standard results processing procedure.

In this study, the experimental setup for the electron paramagnetic resonance spectroscopy (EPR) measurements were performed on EPR spectrometer Radiopan 2547 SE/X, equipped with resonator type RCX660A, electromagnet device ER 2505 and corresponding high-frequency unit MS212 with frequency of 9.3 GHz. Experimental measurements of electronic paramagnetic resonance (EPR) spectral transition line parameters were performed by using the EPR spectrometer equipped with a TE type resonant cavity. In measuring temperature dependences in the range from 77 to 300 K, the cryostat module of liquid nitrogen can be used [13; 20; 23; 24]. The changes in spectral features were measured using an EPR spectrometer under appropriate experimental conditions, settings and modes setup.

Results

The dependences of the intensity of the EPR absorption spectra for the initial Yb_2O_3-CeO_2 ytterbium oxide powder and the ceramic samples obtained at both temperatures selected for the experiment [12-16] are presented in Figure 1. The measurement results indicate a considerable effect of the treatment temperature of Yb_2O_3-CeO_2 samples on their spectroscopic features. The obtained EPR spectra were analysed for each sample; the measurement results were subject to high-quality integration [14-16]. The width and the centre of the lines show the offset for each sample, and, in general, correspond to the expected. Intensities and area under the curve increase for both heat-treated samples (Figure 2). For the studied samples, the experimental results agree well with the theoretical Lorentz model. The quality and measurement procedure [17-19], interpolation and compliance with the Lorentz theoretical model are proved by the value of Adj. R-square, which is equal to 0.99.

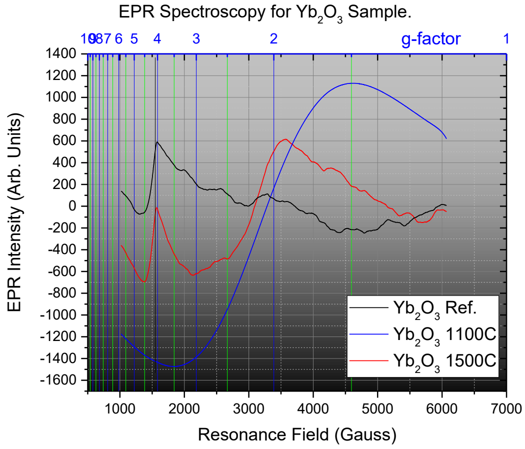

Figure 1. EPR absorption lines of Yb_2O_3 for processing temperature Ref. -1100 °C -1500 °C

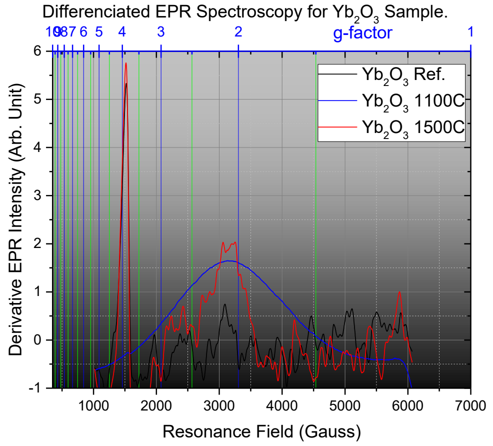

Figure 2. Derived from Yb_2O_3 spectroscopic EPR lines and spectral features for different processing temperatures Ref. -1100 °C -1500 °C

EPR characteristic of the initial Yb_2O_3 powder and ceramics based on REOs. The dependences of the intensity of the EPR absorption spectra for the initial Yb_2O_3 powder and the ceramic samples obtained at both temperatures selected for the experiment are shown in Figure 1. The EPR spectra demonstrate changes in the intensity of the transmission lines which indicates changes in properties and parameters of the Yb_2O_3 oxides. High temperature treatment of the Yb_2O_3 oxides shows redistribution in the spectral parameters along the spectral range of the EPR spectra. Emergence of the additional spectral lines between main two phases of the Yb_2O_3 oxide indicates fine structures formation. Initial state of the REO oxides is mostly in paramagnetic region with g-factors close to 4 that is common to the most nonmagnetic materials. The minimal presents of the ions in the region of g-factor of

2 indicates form of the oxide. Temperature treatment of 1100 °C leads to increase in more ferromagnetic parameters of the Yb_2O_3 oxide in region with g-factor equals to 2. This fact means the ferromagnetic properties dominates for this form of the oxide. High temperature treatment of 1500 °C leads to increase both in paramagnetic and in ferromagnetic parameters of the Yb_2O_3 oxide in region with g-factor equals to 4 and 2, accordingly. This fact is presented in Figure 1 and indicates partial domination of the paramagnetic form of the oxide. This form of the oxide includes both paramagnetic and ferromagnetic properties of the oxide in the material. This implies emergence both paramagnetic ions and ferromagnetic ions in the appropriate form of the material. The FWHM of the transition line g-factor of 4 remain constant for paramagnetic parameters which implies no phase changes in the form of the Yb_2O_3 oxide.

The FWHM of the transition line with g-factor of 2 demonstrates considerable changes for ferromagnetic parameters and implies formation of the new form of the oxide. This fact adds significant meaning to the interpretation and attribution of the physical and chemical mechanisms of the new oxide form formation under high temperature treatment of the REOs oxide materials. The area under the curve can also indicate changes in number of ion and spins that are in the appropriate form of the oxide along the spectral range. This parameter is clearly demonstrating the new form of the oxide with g-factor of 2 for the FWHM of the transition line of the Yb_2O_3 oxide. Additional heat treatment 1500 °C leads to existence of both ferromagnetic and paramagnetic forms of the oxides. The FWHM of the both oxide form returns to two lines forms and remains close to the FWHM of the initial base form of Yb_2O_3 oxide. The area under the curve can be the one of the important parameters to find and indicate changes in oxide formation of the form of the oxide REO material. Features and parameters that indicate changes in oxide form include the area under the curve, the resonance field, full width at half maximum and intensity of the spectral line of the oxide material. Theoretical model can be additional factor to indicate changes in the form of the oxide form REO material. Additional spectral parameter is present close to g-factor 1.25, which is attributed to the formation of the additional phase of the oxide. On the spectra graph it is shown this spectral line that is attributed to the physical mechanism in the text below. The measurement results indicate a significant effect of the high temperature treatment of Yb_2O_3 samples on their spectroscopic features. The obtained EPR spectra were analysed for each sample; the measurement results were subject to high-quality integration [18-20].

The width and centre of the lines show the offset for each sample, and, in general, correspond to the expected results. Intensities and area under the curve represented in Figure 2 increase for both heat-treated samples. The quality and measurement procedure [13; 16; 25], interpolation and compliance with the Lorentz theoretical model are proved by the value of Adj. R-square, which is equal to 0.99.

For the input sample (T=120 °C) in the EPR spectrum, lines were found at 1508 G and 3502 G, which characterise the corresponding oxides of CeO_2 and Yb_2O_3 with a factor of 3,893 and 2,025, respectively. In the sample of ceramics obtained at T=1100 °C, changes in the intensity and width of the spectral line of the oxide Yb_2O_3 were detected. The above changes correspond to the emergence in the EPR spectrum of the Yb^{3+} cation line with unchanged features of cerium oxide at 1550 G. In the sample with heat treatment at 1100 °C there are EPR lines for Yb_2O_3 found lines at 1508 G and 3502 G with g-factor values of 3,893 and 2,025, respectively. These lines correspond to finding the ground position for the Yb^{3+} ion. The similar arrangement of the line and its shape indicates the emergence of monoclinic ytterbium oxide for a factor with a value of 2,025. The same conclusion can be obtained for the second main line of the EPR with a factor value of 3,893.

In the sample (1500 °C within 10 h) in the treated EPR spectrum for Yb_2O_3 there are lines 1316 G, 1508 G 1725 G, 1951 G, 2236 G, 2422 G, 2755 G, 3057 G, 3242 G with the corresponding values of g-factor 4.31, 3,893, 3,478, 3,144, 2.82, 2,637, 2,362, 2,138, 2,025. In the sample (1500 °C within 50 h) in the treated EPR spectrum for Yb_2O_3, there are lines 3911 G, 4196 G, 4456 G, 5084 G, 5495 G, 5854 G with the corresponding values of g-factor 1.72, 1,611, 1,522, 1,354, 1,254 and 1,188. In this case, the presence of several phases in Yb_2O_3 in the corresponding phase form was determined.

Figure 3 demonstrates the intensity of the line at 1508 G is maximal and corresponds to the emergence in the spectral features of the Ce^{3+} cation sample. The EPR spectrum also indicates a 3502 G line corresponding to the Yb^{3+} ion, and a new 5495 G line has appeared, which characterises the transition of the Yb ion to a new form and the possible phase conversion of cubic Yb_2O_3 oxide to monoclinic. Changes in the EPR spectrum after heat treatment at T=1500 °C correspond to the presence of most of the spins of the sample in the spectral state with an energy of 1508 G. The spectra also contain spins in the spectral state with energies of 3502 G and 5495 G.

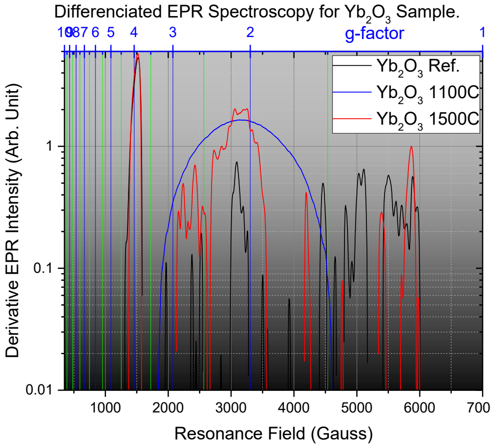

Figure 3.Derived from Yb_2O_3 spectroscopic EPR lines and spectral features for different processing temperatures Ref. -1100 °C -1500 °C

The intensity dependence of the experimental EPR lines measured for Yb_2O_3 samples fully corresponds to the Lorentz theoretical model shown in Figure 4. Characteristic spectral parameters, such as the width, centre, and shape of the EPR lines, show changes within the Knight’s shift. The height of the lines and the area under the curves of the calcined Yb_2O_3 samples indicate a linear increase in the structural rearrangement, accompanied by an increase in the number of magnetic domains.

Two lines corresponding to the ions of ^{155}Yb and ^{157}Yb isotopes were found in the EPR spectra at the frequency of the g-factor value of 1,991. There are also lines in the spectrum that, for Yb^{3+} ions correspond to cubic and monoclinic systems. Figure 4 demonstrates an increase in the calcination temperature is accompanied by an increase in the g-factor and a corresponding shift of the spectral line towards smaller magnetic fields.

Figure 5 demonstrates lines with g-factor values of 3,478 and 1,427 correspond to the cubic phase of Yb_2O_3 oxide. The intensity of the lines with this g-factor dominates in the spectrum of these oxide samples (Table 1). These lines are in the spectrum at 1725 G and 4808 G on the resonant field scale in the EPR spectrum. In this case, the Yb^{3+} ion takes the form of the main ion in the crystal of this oxide based on (REOs).

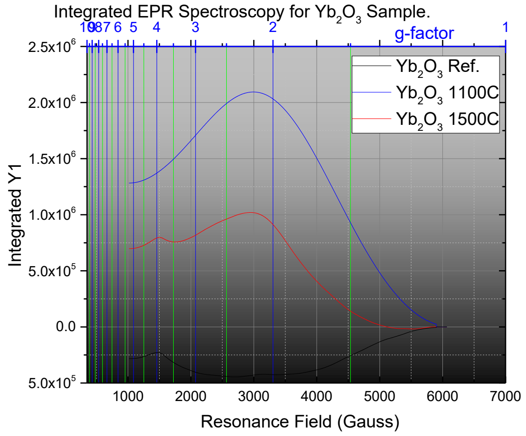

Figure 4. Integrated lines of EPR spectra of Yb_2O_3 samples and their correspondence Lorentz theoretical model

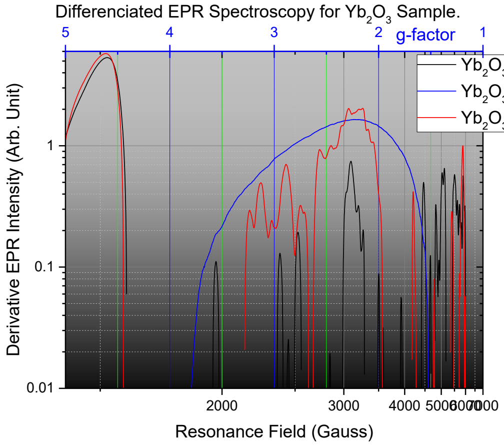

Figure 5. Integrated lines of EPR spectra of Yb_2O_3 samples in g-factor representation

Table 1. Spectral features of samples based on oxides of rare earth elements (REO) with Hc (Gauss) and g-factor parameters for heat treatment at Ref., 1100 °C, 1500 °C

	g-CeO_2	RF-CeO_2	g-Yb_2O_3	RF-Yb_2O_3	g-Yb_2O_3-CeO_2	RF-Yb_2O_3-CeO_2
	g-factor	Hc (Gauss)	g-factor	Hc (Gauss)	g-factor	Hc (Gauss)
1	3.96	1557	4.31	1316	5.23	1023
2	4	1462	3,893	1508	3.71	1592
3	4.35	1371	3,478	1725	2.96	2120
4	4,215	1426	3,144	1951	2.62	2488
5	3.76	1656	2.82	2236	2,276	2848
6	3.32	1930	2,637	2422	2,097	3133
7	3.01	2172	2,362	2755	2.03	3250
8	2.45	2775	2,138	3057	1.97	3359
9			2,025	3242	1,907	3476
10			1.88	3502	1,522	4465
11			1.72	3911	1,419	4808
12			1,611	4196	1,329	5176
13			1,522	4456	1,304	5276
14			1,354	5084	1,279	5378
15			1,254	5495	1,234	5595
16			1,188	5854	1.17	5921

EPR characteristic of the initial CeO_2 powder and ceramics based on REOs. Characteristic spectral lines corresponding to the presence of Ce^{3+} ions with a characteristic line at 1550 G with a g-factor of 4.4 are found in the EPR spectrum and is shown in Figure 6. The corresponding value of the resonant field 1550 G, line width and line shape indicate the emergence of a line of cerium oxide CeO_2 in the spectrum in the main sample. The position of the line characterises the magnetic component of this sample CeO_2 with a g-factor of 4.4. The line width corresponds to a value of 40 G and means the ionic characteristic of the corresponding line with a value of Ce^{3+}.

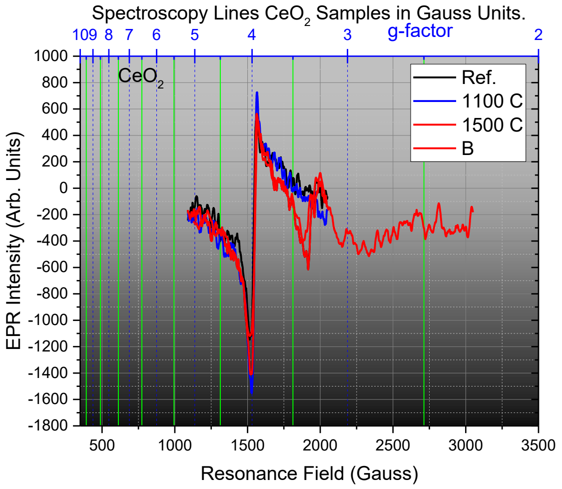

Figure 6. EPR absorption lines for a CeO_2 mixtures and ceramics based on REO

For the Figure 7 with the spectrum of the derivative for the corresponding CeO_2 sample, the values of the g-factor and the values of the resonant field of the EPR spectrum are given. The corresponding EPR lines of the spectrum are determined by the higher resolution and the ratio of the EPR signal to the noise component. The line width is measured according to the standard results processing procedure for the corresponding line and mathematical model. The line intensity derivative is proportional to the EPR line intensity and corresponds to the magnetic susceptibility of the sample. The value of H height of the spectroscopic EPR line means the number of spins in this state with a given g-factor under the same experimental conditions.

For the CeO_2 sample, the values of g-factor before and after heat treatment are given with a value of 4.4 for the main line and 3.8 for the line after treatment at 1500 °C. The EPR spectrum also contains 2400 G spectral lines with a g-factor of 3.0 and a 2600 G line with a g-factor of 2.5, which are characterised by a minimum value of intensity relative to the main lines. Note that most of these lines are absent in the composite oxides based on CeO_2 and have minimal effect on the spectral, magnetic, and ionic features of the samples. The shape of the EPR line characterises the corresponding theoretical Lorentz model for mathematical processing of the corresponding line or the corresponding set of spectral lines represented in Figure 8.

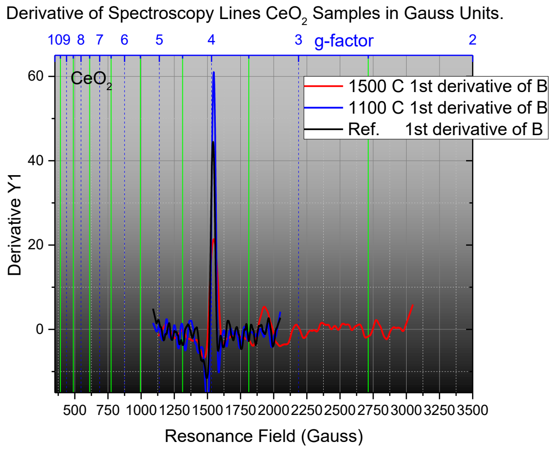

Figure 7a. Derived EPR absorption lines for a CeO_2 mixture and ceramics based on REO

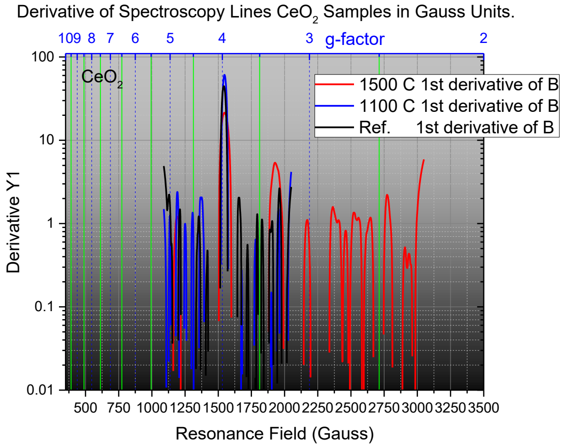

Figure 7b. Derived EPR absorption lines and spectral features for a CeO_2 mixture and ceramics based on REO

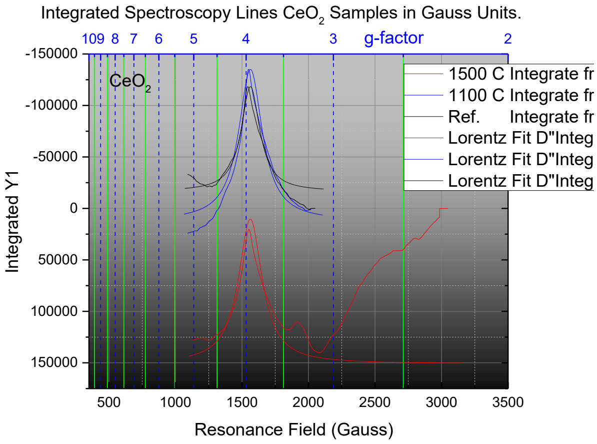

Figure 8. EPR absorption lines for CeO_2 mixture and ceramics based on REO and their compliance with the theoretical Lorentz model

Figure 8 with the EPR spectra demonstrates the integral intensity and spectral lines with the corresponding values of the resonant field and the g-factor for the CeO_2 sample. The presented lines are processed using a theoretical Lorentz mathematical model. Figures 7a and Figure 7b show the changes in the intensity of the main line at 1550 G with a g-factor of 4.4 at a temperature treatment of 0 to

1500 °C. It is shown that heat treatment leads to changes in the intensity of the corresponding EPR lines. Processing of the sample at 1100 °C leads to increase in the intensity of the main line by 30%. Treatment of cerium oxide at 1500 °C leads to decrease in the intensity of the main line of CeO_2 by 50% and the emergence of additional spectral lines at 1900 G and 2500 G with g-factor values of 3.8 and 3.0. These lines correspond to the additional emergence of cerium oxides of CeO_2 ion form in the internodes [110] and [11¯0]. The emergence of Ce^{3+} substitution ions in the crystal lattice with a g-factor of 2.5 and a resonant field at 2750 G is possible.

The emergence of additional spectral lines is accompanied by a decrease in the intensity of the main line by 1550 G with a g-factor of 4.4. The coefficient of reduction of the intensity of the main line and the relative intensity of the additional spectral lines after thermal treatment demonstrates the conservation law for the total number of spins in different oxide forms. The law of conservation of the number of spins allows finding additional spectral lines that appear during heat treatment for cerium oxides CeO_2 or changes in the external factor of oxide treatment.

Characterisation of CeO_2-Yb_2O_3 ceramics by EPR spectroscopy. In the EPR spectrum of Yb_2O_3 oxide in CeO_2, spectral transition lines with a resonant field value at 1550 G with a g-factor of 4.45 were additionally found. The spectral line is present and increases with the corresponding spectral processing temperature by a factor of 10 from 1100 °C to 1500 °C. The position of this line and the absence of a line with a g-factor of 3.4 in the spectrum mean that the line belongs to the oxide Yb_2O_3.

A set of lines with a resonant field of 2700 G, 3200 G and 3500 G, corresponding to the values of g-factor 2.5, 2.25 and 1.99, was also found and measured in the spectrum in Figure 9. Lines with such g-factor values are absent in the spectrum of pure CeO_2 oxide, which means the presence of lines with such g-factors in the Yb_2O_3 spectrum. The presence of several lines in the EPR spectrum with a g-factor of 2.0-2.5 means the presence of two or more phases of Yb_2O_3 oxide in CeO_2. Changes in intensity during heat treatment correspond to an increase or decrease in the concentration of the corresponding oxide phase depending on the temperature. According to the spectral features in the initial sample there are lines expressing the basic form of the oxide with a g-factor of 2.25. After heat treatment of 1100 °C, the corresponding changes in the EPR spectrum are presented, stating the emergence of several lines with a g-factor of 2.5, 2.25 and 1.9. Heat treatment at 1500 °C leads to an increase in the intensity of the EPR line and the transition of the oxide to the main position of the line with a g-factor of 2.25.

Figure 9 demonstrates the EPR spectral lines at 4750 G, 5000 G, 5300 G, and 6000 G, which refer to the g-factor values of 1.44, 1.25, 1.15, and 1.1, respectively. Such changes in the EPR spectra indicate the emergence and redistribution of the phase structure of Yb_2O_3 oxide. Spectral lines with a g-factor of 4.45 and 2.45 correspond to the cubic form of Yb_2O_3-CeO_2 oxide with Yb^{3+} ion. In the main sample of Yb_2O_3-CeO_2 oxide, the spectral lines with g-factor 4.45 and 2.25 correspond to the single-crystal form with the Yb^{3+} ion. The sample of Yb_2O_3-CeO_2 oxide also has a minimum amount of single crystal with spectral lines 4800 G, 5300 G, and 6000 G with a g-factor of 1.5, 1.25, and 1.1, respectively.

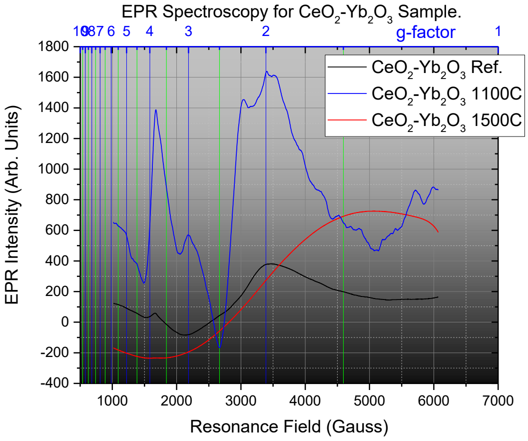

Figure 9. EPR absorption lines for the mixture Yb_2O_3-CeO_2.at the processing temperature Ref.-1100 °C-1500 °C

Upon 1100 °C heat treatment, sample spectral features demonstrate a decrease in the concentration of the single-crystal oxide form with a g-factor of 4.45 and the emergence of lines with a g-factor of 2.45, which corresponds to the emergence and dominance of the cubic form of ceramic. During heat treatment of 1500 °C in the EPR spectrum, the spectral lines show the dominance of lines with a g-factor of 2.25 which correspond to the emergence of the trigonal phase of Yb_2O_3 oxide. Figure 10a demonstrates that spectral lines corresponding to the cubic form of Yb_2O_3 oxide disappear or significantly decrease.

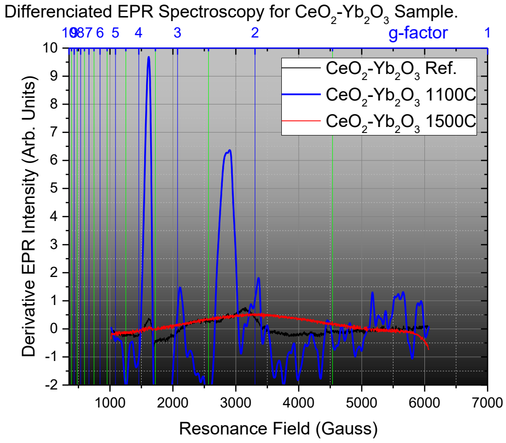

Figure 10a. Derived from Yb_2O_3-CeO_2 spectroscopic EPR lines for different processing temperatures Ref.-1100 °C-1500 °C

In Figure 10b, the lines found in the EPR spectra indicate that the lines with a factor of 1.323, 1.421, 4.31, and 1.522 correspond to the trigonal phase of the oxide Yb_2O_3-CeO_2. These lines are in the spectrum at 5176 G, 4808 G, 1316 G and 4465 G on the resonant field scale in the EPR spectrum. EPR lines corresponding to a factor of 2.96, 3.71, 2.62, 5.23, 1.234 also belong to the trigonal form of the oxide Yb_2O_3-CeO_2. These lines are in the spectrum at 2120 G, 1592 G, 2488 G, 1023 G, and 5595 G on the resonant field scale in the EPR spectrum.

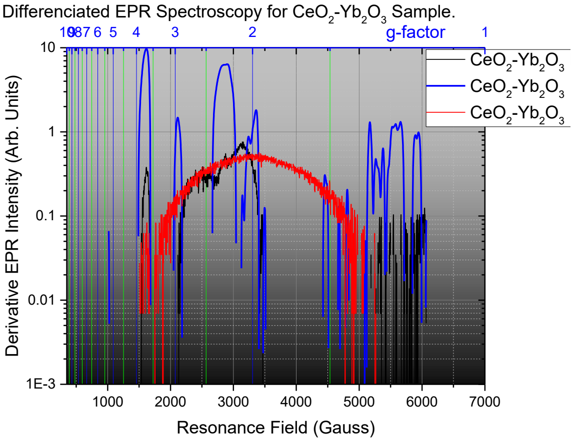

Figure 10b. Derived from Yb_2O_3-CeO_2 spectroscopic EPR lines and spectral features for different processing temperatures Ref.-1100 °C-1500 °C

The transmission lines with g-factor values of 2.030 and 3.891 correspond to the cubic phase of Yb_2O_3-CeO_2 oxide, which is presented in Figure 11. The intensity of the lines with this g-factor dominates in the spectrum of these oxide samples. These lines are in the spectra at 1592 G and 3250 G on the resonant field scale in the EPR spectrum. In this case, as Figure 12 demonstrates, the Yb^{3+} ion takes the form of the main ion in the crystal of this oxide based on (REOs).

Discussion

Recently some of the researches have been done on the CeO_2 oxides [22]. For example, heterostructured CeO_2-M (M=Co, Cu, Mn, Re, Ni) oxide nano-catalysts are described in [26]. In addition, how environmentally relevant UV-A exposure affect the toxicity of cerium oxide and CeO_2-based nanostructure materials is considered and represented in [22]. The comparison of the results with the research achieved by other investigators conclude that this result is close to the result obtained on the similar objects (Cu-CeO_2) by investigations, see [27]. At the same time, it possible to conclude that our results are unique and does not always coincide with the EPR investigations on similar objects [21].

The features of EPR for Yb_2O_3-CeO_2 samples were processed and analysed by means of the EPR spectroscopy. The features of the spectra indicate the presence of EPR spectral transition lines for Yb_2O_3 and correspond to the number of ions of the corresponding material. The intensity of the EPR lines corresponds to the emergence of spins in the appropriate form. The value of the resonant field characterises the form of the corresponding spin. The integrated spectral characteristic also corresponds to the number of oxide spins in the corresponding Yb_2O_3-CeO_2 mixture. The EPR Intensity is responsible for the magnetic susceptibility for a given Yb_2O_3-CeO_2 oxide material. The value of the resonant field is responsible for the magnetic features of the corresponding mixture. The width of the spectral line (FWHM) determines how much of this sample mixture is presented in the form of a ferromagnet. The differential characteristic determines the emergence of this ion in this form of the oxide. The characteristic determines the ionic features of the mixture of Yb_2O_3-CeO_2 oxide material. Confirmation of the hypothesis in this mixture of Yb_2O_3-CeO_2 is indicated in the fact that within the theoretical Lorentz model it is possible to measure and perform studies with complex processing of EPR spectroscopy results.

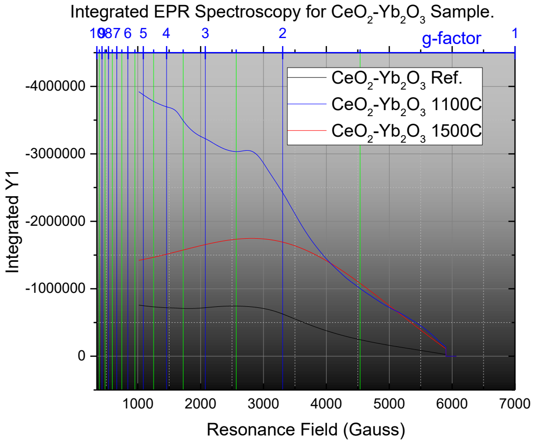

Figure 11. Integrated lines of EPR spectra of Yb_2O_3 Yb_2O_3-CeO_2 samples and their correspondence Lorentz theoretical model

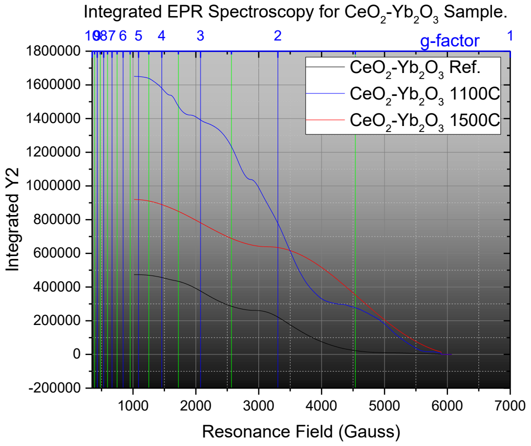

Figure 12. Integrated lines of EPR spectra of Yb_2O_3 Yb_2O_3-CeO_2 samples and their correspondence Lorentz theoretical model

Within the framework of this model, it is possible to further investigate the emergence of Chemical and Knight's shift in the spectral EPR features. Appropriate study and interpretation make it possible to investigate changes in the chemical composition of the phase transformation of the emergence of a mixture, the conversion of ions or the physical conversion of Yb_2O_3-CeO_2 oxide into another form of crystal structure. The physical transformations correspond to an additional model of shifts in the spectral EPR range. The prospect of processing the results of EPR spectroscopy using a mathematical physical model allows measuring the process and interpreting the features and parameters of the material. The hypothesis of interpretation of EPR spectra using the mathematical Lorentz model is confirmed on samples of mixtures of oxides based on Yb_2O3-CeO_2 for REO oxides of rare earth elements.

Conclusions

The electron paramagnetic resonance spectroscopy (EPR) spectra for oxides (REOs) show that during thermal treatment of samples from 120 °C to 1500 °C, changes in intensity, position of spectral lines, changes in the value of g-factor and changes in the shape of the corresponding curves in the spectrum were found. Thermal treatment of oxide samples leads to redistribution in the spectral EPR features and properties of oxides and the dominance of features with the corresponding discrete and continuous values. The correspondence of the theoretical model of the magnetic properties of CeO_2 samples in a wide range of experimental conditions was shown. For experimental data, the dependence of the intensity of the EPR line is in good accordance with the theoretical models. Features for CeO_2 samples such as line width, line centre, EPR line shape remain unchanged. While the height of the line, the area under the curve shows a linear increase with the value (Receiver Gain) of the amplitude of the gain.

The intensity dependence of the experimental EPR lines measured for Yb_2O_3 samples fully corresponds to the Lorentz theoretical model. Characteristic spectral parameters, such as the width, centre, and shape of the EPR lines, show changes within the Knight’s shift. The height of the lines and the area under the curves of the calcined Yb_2O_3 samples indicate a linear increase in the structural rearrangement, accompanied by an increase in the number of magnetic domains. Lines with g-factor values of 3,478 and 1,427 correspond to the cubic phase of Yb_2O_3 oxide. The intensity of the lines with this g-factor dominates in the spectrum of these oxide samples. These lines are in the spectrum at 1725 G and 4808 G on the resonant field scale in the EPR spectrum. In this case, the Yb^{3+} ion takes the form of the main ion in the crystal of this oxide based on (REOs). The EPR spectra of the initial mixture of oxides of Yb_2O_3-CeO_2 and ceramics based on them show changes in the spectroscopic features of oxide Yb_2O_3-CeO_2 and the form of cations Yb^{3+} with factor 2, which correspond to the phase transition of the two-phase system of faceted and centred cubic ytterbium oxide (Ref.-120 °C) in a three-dimensional centred cubic sample of ceramics at T=1100 °C and, further, the transition of the specified cubic sample in a monoclinic system at T=1500 °C.

References

[1] Ivanov VK, Shcherbakov B, Usatenko AV. Structurally sensitive properties and biomedical application of nanodispersed cerium dioxide. *Adv. Chem.* 2009;(78):924-37.

[2] Li H, Xia P, Pan S, Qi Z, Fu Ch, Yu Z, et al. The advances of ceria nanoparticles for biomedical applications in Orthopaedics. *Int. J. Nanomedicine.* 2020;(15):7199-214.

[3] Wang F, Xu L, Yang J, Zhang J, Zhang L, Li H, et al. Enhanced catalytic performance of Ir catalysts supported on ceria-based solid solution for methane dry reforming reaction. *Catal. Today.* 2017;(281):295-303.

[4] Han D, Yang Y, Gu F, Wang Z. Tuning the morphology and upconversion fluorescence of CeO_2: Er/Yb Nanooctahedra. *J. Alloys Compd.* 2015;(656):524-29.

[5] Wang B, Zhu B, Yun S, Zhang W, Xia Ch, Afzal M, et al. Fast ionic conduction in semiconductor $CeO_{2-\delta}$ electrolyte fuel cells. *NPG Asia Mater.* 2018;(51):1-12.

[6] Ping L, Xiaoyin Ch, Yongdan L, Johannes SW. A review on oxygen storage capacity of CeO_2-based materials: Influence factors, measurement techniques, and applications in reactions related to catalytic automotive emissions control. *Today.* 2018;(327):90-115.

[7] Maksimchuk PO, Seminko VV, Bespalova II, Masalov AA. Influence of size of CeO_2 nanocrystals on the processes of vacancies formation determined by spectroscopic techniques. *Funct. Mater.* 2014;21(3):254-59.

[8] Anirban SK, Dutta A. Revisiting ionic conductivity of rare earth doped ceria: Dependency on different factors. *Int. J. Hydrog. Energy.* 2020;45(46):25139-166.

[9] Kornienko OA, Andrievskay OR, Barshchevskaya HK. Phase relations in the system ternary based on Ceria, Zirconia and Ytterbia at 1500 °C. *J. Chem. Technol.* 2020;(2):142-52.

[10] Andrievskaya ER, Kornienko OA, Sameljuk AV, Bykov AI. Interaction of Ceria and Ytterbia in air within temperature range 1500-600 °C. *J. Eur. Ceram. Soc.* 2019;39(9):2930-35.

[11] Schmitt R, Nenning A, Kraynis O. A review of defect structure and chemistry in ceria and its solid solutions. *Chem. Soc. Rev.* 2020;(49) 554-92.

[12] Coduri M, Checchia S, Longhi M, Ceresoli D, Scavini M. Rare Earth doped Ceria: The complex connection between structure and properties. *Front. Chem.* 2018;(6):article number 526. https://doi.org/10.3389/fchem.2018.00526.

[13] Bataiev MM, Bataiev YM, Lavrynenko OM, Kornienko OA. Surface magnetic properties and magnetisation dynamics of magnetite nanoparticles doped with platinum ions. *Nanosystems. Nanomaterials. Nanotechnologii.* 2020;18(2):311-20.

[14] Dubowski JJ, Geohegan D.B., Kabashin AV, editors. Synthesis and Photonics of nanoscale materials XVII. San Francisco: SPIE; 2020. Vol. 11269, Popova-Kuznetsova E, Tikhonowski G, Popov AA, Duflot VR, Deyev SM, Klimentov SM, Zavestovskaya IN, Prasad PN, Kabashin AV, Colloidal samarium oxide nanoparticles prepared by femtosecond laser ablation and fragmentation for nuclear nanomedicine; article number 1126904. https://doi.org/10.1117/12.2551432.

[15] Anwar MS, Kumar S, Arshi N, Ahmed F, Seo YJ, Lee CG, Koo BH. Structural and optical study of samarium doped cerium oxide thin films prepared by electron beam evaporation. *J. Alloys Compd*. 2011;(509):4525-529.

[16] Lavrynenko OM, Bykov OI, Bataiev YM, Bataiev MM, Kornienko OA. [Influence of temperature on the formation of structures in the CeO_2-Yb_2O_3 system]. *Odesa National University Herald. Chemistry.* 2020;3(75):76-85. Ukrainian.

[17] Farle M. Ferromagnetic resonance of ultrathin metallic layers. Rep. Prog. Phys. 1998;61(7):755-826.

[18] Alonso PJ, Alcalá R, Usón R, Forniés J. EPR study of mononuclear Pt(III) organometallic complexes. *J. Phys. Chem*. Solids. 1991;52(8):975-78.

[19] Kaufmann U. EPR and optical absorption of Fe^+, Fe^{2+}, Fe^{3+}, and Fe^{4+} on tetragonal sites in $CdSiP_2$. *Phys. Rev. B.* 1976;14(5):1848-50.

[20] Samsonov GV, Vlasova MV, Kakazey NG, Grigorjev B, Uskoković D, Ristić M. Study of elementary mechanisms during sintering of MgO with Mn_2O_3, MnO_2, and NiO additive. *J. de Physique.* 1976;37(12):C7-415.

[21] Khan ME, Khan MM, Cho MH. Ce^{3+}-ion, surface Oxygen vacancy, and visible light-induced photocatalytic dye degradation and photocapacitive performance of CeO_2 – graphene nanostructures. *Sci. Rep.* 2017;(7):article number 5928. https://doi.org/10.1038/s41598-017-06139-6.

[22] Jemec A, Djinović P, Gasan I, Črnivec O, Pintar A. The hazard assessment of nanostructured CeO_2-based mixed oxides on the zebrafish Danio rerio under environmentally relevant UV-A exposure. *Sci. Total Environ.* 2015;(506-507):272-8.

[23] Kakazei NG, Sorin LA. The nature of the change in the EPR spectrum of Mn: MgO due to a defect in the crystal structure. *Ukr. Phys. Journal.* 1971;15(11):1903-904.

[24] Samsonov GV, Kakazey NG, Sorin LA. The radio spectroscopic study of defects in crystalline structure. *Phys. Sintering.* 1973;5(3):97-114.

[25] Vlasova MV, Kakazei NG, Kalinichenko AM, Litvinenko AC. Radiospectroscopic properties nonorganic materials. Kyiv: Naukova Dumka; 1987. 718 p.

[26] Mavuso MA, Makgwane PR, Ray SS. Heterostructured CeO_2-M (M=Co, Cu, Mn, Fe, Ni) Oxide Nanocatalysts for the Visible-Light Photooxidation of Pinene to Aroma Oxygenates. *ACS Omega.* 2020;(5):9775-88.

[27] Wang F, Büchel R, Savitsky A, Zalibera M, Widmann D, Pratsinis SE, Lubitz W, Schüth F. In situ EPR study of the redox properties of CuO-CeO_2 catalysts for the preferential CO oxidation (PROX). *ACS Catal.* 2016;6(6):3520-30. https://doi.org/10.1021/acscatal.6b00589.

ЕПР-спектральні, магнітні та іонні характеристики порошків CeO_2, Yb_2O_3, Yb_2O_3-CeO_2 та кераміки на їх основі

Юрій Михайлович Батаєв, Микола Миколайович Батаєв,
Оксана Олександрівна Корнієнко, Олена Михайлівна Лавриненко, Олеся Юріївна Павленко
Інститут проблем матеріалознавства імені Францевича НАНУ
03142, вул. Крижанівського, 3, м. Київ, Україна

Анотація

Актуальність. Природа та властивості рідкісноземельних оксидів впливають на динаміку намагнічування та поверхневі магнітні властивості отриманих керамічних матеріалів. Лінії електронного парамагнітного резонансу та зміни їх інтенсивності допомагають зрозуміти фізичні та хімічні перетворення оксиду в процесі термічної обробки. Вони також визначають відповідну іонну форму, кристалічну форму оксиду та магнітні характеристики.

Мета. Вивчити механізм утворення парамагнітних центрів (з використанням іонів Yb^{3+} та Ce^{4+}), а також вивчити вплив температури на процеси термогенерації.

Методи. Використано метод спектроскопії електронного парамагнітного резонансу. Математична обробка лінії рідкісноземельних оксидів показана за допомогою теоретичної моделі Лоренца.

Результати. Спектри електронної парамагнітної резонансної спектроскопії для задніх оксидів показують, що термічна обробка від 120 °C до 1500 °C призводить до зміни інтенсивності, зміни положення спектральних ліній та модифікації значення g-фактора. Термічна обробка зразків оксидів призводить до перерозподілу спектральних характеристик електронного парамагнітного резонансу та властивостей оксидів і домінування характеристик із відповідними дискретними та безперервними значеннями.

Висновки. Висота ліній та площа під кривими прожарених зразків Yb_2O_3 демонструють лінійне збільшення структурної перестановки разом із збільшенням числа магнітних доменів. Спектри електронного парамагнітного резонансу вихідної суміші оксиду Yb_2O_3-CeO_2 показують зміну спектроскопічних характеристик та форми катіонів Yb^{3+}

Ключові слова: діоксид церію, оксид ітербію, кераміка на основі РЗЕ, спектроскопія ЕПР, динаміка намагніченості, поверхневі магнітні властивості